An analytical calculation method of 3 base fluids suspend by CNTs hybrid nanoparticle over a vertical circular cylinder with sinusoidal radius

M. Gholinia*, D.D. Ganji

Mechanical Engineering Departemnt, Babol Noshirvani University of Technology, P. O. Box 484, Babol, Iran

*Corresponding author, E-mail: M.gholinia1371@gmail.com (M.gholinia)

Abstract:

In this research, the specification of 3-dimensional flow stagnation point of hybrid Nano fluids passing through circular cylinder with sinusoidal radius are analyzed. $C_2H_6O_2$, H_2O and Engine oil are used as an ordinary liquid, while nano-particles include SWCNT and MWCNT. Fluid stream is taken into account with/without considering the effect of thermal slippage. Higher order non-linear phrases are transformed to ordinary prime-order differential equations and then solved applying the Analytical Method (HPM) in Matlab-14 software. Graphical analysis of the impressive parameters like: Prandtl number, thermal slip parameter, CNTs volume fraction is precisely checked on the profiles of velocity and temperature for various carbon nano-tubes. Consequences display that: cooling process or heat transfer rate can be increased by employing smaller thermal slippage parameter. Further, due to the better thermal conductivity of SWCNT carbon nanotube, the temperature increase in these carbon nanotubes is more than that of MWCNT.

Keywords: *Hybrid Nanofluids; Circular cylinder; SWCNT and MWCNT; Thermal slip; HPM method*

1. Introduction:

Recent studies reveal that some carbon structures have very good thermal conductivity. Therefore, diverse studies have been carried out on the thermal properties of Nano fluids using carbon Nano structres such as graphite, single-walled carbon nano-tubes (SWCNT), multi-walled carbon

nano-tubes (MWCNT), Nano-diamonds and graphene [1-8]. Carbon nano-tubes with only one graphene layer are called single-walled carbon nanotubes, while nanotubes with more than one graphene layer are described as multi-walled nanotubes that can slip into one another. The unique characteristics of these materials as a new form of carbon material include strength, hardness, adhesion, chemical stability, thermal conductivity and more interesting than all electrical conductivity, and they have many applications in microelectronics and Nano electronics, fuel storage, preparing flat panel display, constructional composite materials, anti-deposition paint, H_2 storage, radar absorber coating, technical tissues, conductive plastics, improved lifetime batteries, super-capacitors, super strong fibers, biomass sensors for harmful gases, etc. Iijima [9] began investigating carbon nanotubes. Experimental research on MWCNT–H_2O nanoliquid stream and heat transfer in the heat exchanger with cancellous media has been practiced out by Moradi et al. [10]. Application of retrievable carbon nanotube Nano fluids in solar desalination system is examined by Chen et al. [11]. In the similar paper, the influence of surfactants on the resistance and solar thermal sorption specifications of multi-walled carbon nanotubes Nano fluids is discussed by Choi et al. [12]. Selimefendigil and Öztop [13] investigated the MHD free convection of CNT-H_2O nanoliquid in a cavity with a corrugated partition. Also, the use of carbon nanotube Nano fluid in increasing the efficiency of discharged tube solar collector studied by Mahbubul et al. [14]. Effect of magnetic and non-magnetic nanoparticles on mixed convection flow of a new thermal conductivity model with Cu-Fe_3O_4 hybrid nanoliquid over a straight stretching plate has been done by Hussanan et al. [15]. The output of this essay indicates that liquids based in SA should be used to attain high heat transfer rate. Some other essays about carbon nanotubes nano liquid are in references [16-20].

Hybrid nanofluids are potential fluids that offer better thermal efficiency and thermos-physical properties than basic heat transfer fluids (including mineral oils, water and ethylene glycol) and nanofluids with a single nanoparticle type. Hybrid nanofluid is a new fluid that is made by dispersing two different types of nanoparticles into the heat transfer base fluid. Researchers have shown that hybrid nanofluids can replace conventional coolers, especially fluids that operate at very high temperatures. Hybrid nanoliquid also has a large potential to maintain and absorb energy due to the

unique and special structure of any nanoparticle. Another matter propounded in this essay is the tensile cylinder. Tensile cylinder is increasingly used in the laboratory to investigate the reaction between liquids and solid surfaces. This cylinder often works at high temperature gradients. Recent studies demonstrate the importance of this topic, for example: Numerical check on entropy generation during natural convection of hybrid nanoliquid in a sigmoid passage between straight elliptic cylinders has been done by Tayebi and Öztop [21]. Sundar et al. [22] discussed friction factor and turbulent heat transfer in a horizontal tube of Nano diamond-nickel hybrid Nano fluids flow. Impact of hybrid Nano fluids in solar thermal systems on the proficiency of parabolic trough gatherers is analyzed by Minea and Maghlany [23]. In the similar paper, Bellos and Tzivanidis [24] considered the mono and hybrid Nano fluids for thermal investigate of parabolic trough collector. Entropy generation analysis and heat transfer proficiency in a flat tube of hybrid Nano fluids is addressed by G. Huminic and A. Huminic [25]. Some other activities about hybrid Nano fluids and Nano fluids flow are in references [26-29].

In this research, the aim is to check the characteristics of 3-dimensional flow stagnation point of hybrid nano liquids passing through circular cylinder with sinusoidal radius. The flow regime is considered with both electromagnetic source and the effects of thermal slippage. The potent nonlinear systems calculations are offered using the analytical manner after non-dimensionalization. Plus, graphical analysis of the impressive parameters is precisely checked on the profiles of velocity and temperature for various carbon nano-tubes (SWCNT - MWCNT).

2. Mathematical formulation:

The 3-dimensional stream of hybrid nano fluids is considered as independent of time for a circular cylinder. The cylinder's radius changes sinusoidally. It is substantial to note that at each point M, N and O (utmost and minim radius), there exists an immobility point. The W, V and U are the component of velocities along $Z-$ path, $Y-$ path and $X-$ path respectively. Following us have [30]:

$$u_e^* = a^*X, \quad v_e^* = b^*Y \tag{1}$$

Where a* and b*are free stream affiliate constants. The stream-lines is specified by the equation $X_e^* = \beta 1/c$ where $c = b^*/a^*$, and β is constant which offers a particular stream-line. The appendix-lines of the saddle stagnation point span is $-1 < c < 0$ while the appendix-lines of the nodal stagnation point span is $0 < c < 1$. If $c = 0$ then flow is plane. The stream-lines in this regard are specified in Figure 1(b). The definitive flow narrating equations are [31-32]:

$$\frac{\partial U}{\partial X} + \frac{\partial V}{\partial Y} + \frac{\partial W}{\partial Z} = 0, \tag{2}$$

$$U\frac{\partial U}{\partial X} + V\frac{\partial U}{\partial Y} + W\frac{\partial U}{\partial Z} = a^{*2}X + v_{hnf}\frac{\partial^2 U}{\partial^2 Z}, \tag{3}$$

$$U\frac{\partial V}{\partial X} + V\frac{\partial V}{\partial Y} + W\frac{\partial V}{\partial Z} = b^{*2}Y + v_{hnf}\frac{\partial^2 V}{\partial^2 Z}, \tag{4}$$

$$(\rho C_p)_{hnf}\left(U\frac{\partial T}{\partial X} + V\frac{\partial T}{\partial Y}\right) = K_{hnf}\frac{\partial^2 T}{\partial^2 Z}. \tag{5}$$

The boundary conditions are

$$U = 0, \quad V = 0, \quad W = 0, \quad \gamma k_{hnf}\frac{\partial T}{\partial Z} = T - T_w, \quad \text{when } z = 0 \tag{6}$$

$$U \rightarrow u_e^*, \quad V \rightarrow v_e^*, \quad T \rightarrow T_\infty \quad \text{when } z \rightarrow \infty \tag{7}$$

Where *T, U, V* and *W* are the temperature and speed component along *X, Y* and *Z_* path.

2.1. Properties of Hybrid Nano fluid and model

The nano-particle of SWCNT is combined with the base liquid (Ethylene glycol) to form the Nano fluid. Similarly, for MWCNT. SWCNT combined with MWCNT in the base fluid (Ethylene glycol) to form the Hybrid nano fluid (SWCNT – MWCNT/ Ethylene glycol). For the globular nano-particles, we take the amounts n = 1. The thermosphysical specification of fluid (at ambient temperature) and particles are defined in Table 1.

The general form of the operative thermo-physical specification of Hybrid nano liquid and nano liquid is defined [25, 30].

4

Density

$$\rho_{nf} = (1-\phi)\rho_f + \phi\rho_s, \quad \rightarrow \quad \textbf{Single}$$

$$\rho_{hnf} = \left[\left\{(1-\phi_{SWC})(1-\phi_{MWC})\rho_f\right\} + \phi_{MWC}\rho_{S_{(MWC)}}\right] + \phi_{SWC}\rho_{S_{(SWC)}}, \quad \rightarrow \textbf{Hybrid}$$

Heat capacity

$$(\rho C_p)_{nf} = (1-\phi)(\rho C_p)_f + \phi(\rho C_p)_s, \quad \rightarrow \textbf{Single}$$

$$(\rho C_p)_{hnf} = \left[\left\{(1-\phi_{SWC})(1-\phi_{MWC})(\rho C_p)_f\right\} + \phi_{MWC}(\rho C_p)_{S_{(MWC)}}\right]$$
$$+\phi_{SWC}(\rho C_p)_{S_{(SWC)}}, \quad \rightarrow \textbf{Hybrid}$$

Viscosity

$$\mu_{nf} = \frac{\mu_f}{(1-\phi)^{2.5}}, \rightarrow \textbf{Single} \qquad \mu_{hnf} = \frac{\mu_f}{(1-\phi_{MWC})^{2.5}(1-\phi_{SWC})^{2.5}}, \rightarrow \textbf{Hybrid}$$

$$\frac{k_{nf}}{k_f} = \frac{k_s + (n-1)k_f - (n-1)\phi(k_f - k_s)}{k_s + (n-1)k_f + \phi(k_f - k_s)}, \quad \rightarrow \textbf{Single}$$

Thermal conductivity

$$\frac{k_{hnf}}{k_{bf}} = \frac{k_{S_{(SWC)}} + (n-1)k_{bf} - (n-1)\phi_{SWC}\left(k_{bf} - k_{S_{(SWC)}}\right)}{k_{S_{(SWC)}} + (n-1)k_{bf} + \phi_{SWC}\left(k_{bf} - k_{S_{(SWC)}}\right)}, \qquad \rightarrow$$

$$\textbf{Hybrid}$$

$$\frac{k_{bf}}{k_f} = \frac{k_{S_{(MWC)}} + (n-1)k_f - (n-1)\phi_{MWC}\left(k_f - k_{S_{(MWC)}}\right)}{k_{S_{(MWC)}} + (n-1)k_f + \phi_{MWC}\left(k_f - k_{S_{(MWC)}}\right)}. \qquad \rightarrow$$

The introduction of the similarity transformations [30]:

$$U = a^* X F'(\eta), \ V = b^* Y G'(\eta), \ W = -\sqrt{a^* v_f}\,(F(\eta) + cG(\eta))$$
$$T = T_\infty + (T_w - T_\infty)\Theta(\eta), \quad \eta = Z\sqrt{\left(\frac{v_f}{a^*}\right)}$$

$$(8)$$

Here prime displays derivative to η, δ is thermal slip parameter and c = b*/ a*, G′ (η) and F′ (η) represents the velocity profiles along Y − and X − side respectively, Θ (η) displays the temperature profile.

Reduced Eqs. (2) − (5) to a system of dimensionless nonlinear ordinary differential equations [30]:

$$\dfrac{1}{(1-\phi_{MWC})^{2.5}(1-\phi_{SWC})^{2.5}\left[1-\phi_{SWC}\left((1-\phi_{MWC}+\phi_{MWC}\dfrac{(\rho C_p)_{S_{(MWC)}}}{(\rho C_p)_f})\right)+\phi_{SWC}\dfrac{(\rho C_p)_{S_{(SWC)}}}{(\rho C_p)_f})\right]}F'''$$

$$+cGF''-F'^2+FF''+1=0 \tag{9}$$

$$\dfrac{1}{(1-\phi_{MWC})^{2.5}(1-\phi_{SWC})^{2.5}\left[1-\phi_{SWC}\left((1-\phi_{MWC}+\phi_{MWC}\dfrac{(\rho C_p)_{S_{(MWC)}}}{(\rho C_p)_f})\right)+\phi_{SWC}\dfrac{(\rho C_p)_{S_{(SWC)}}}{(\rho C_p)_f})\right]}G'''$$

$$+FG''+cGG''-cG'^2+c=0 \tag{10}$$

$$\dfrac{\dfrac{k_{hnf}}{k_f}}{Pr\left[1-\phi_{SWC}\left((1-\phi_{MWC}+\phi_{MWC}\dfrac{(\rho C_p)_{S_{(MWC)}}}{(\rho C_p)_f})\right)+\phi_{SWC}\dfrac{(\rho C_p)_{S_{(SWC)}}}{(\rho C_p)_f})\right]}\Theta''+F\Theta'+cG\Theta'=0 \tag{11}$$

Subject to boundary conditions

$$\begin{aligned}
&F(0)=0,\ \ F'(0)=0,\ \ F'(\infty)\to1,\\
&G(0)=0,\ \ G'(0)=0,\ \ G'(\infty)\to1,\\
&\Theta(0)=1+\delta\dfrac{k_{hnf}}{k_f}\Theta'(0),\ \ \Theta(\infty)\to0
\end{aligned} \tag{12}$$

Mathematical statement for heat transfer rate and surface drag force are:

$$C_{fx}=\dfrac{\tau_{WX}}{\rho_f U_W^2},\ \ C_{fy}=\dfrac{\tau_{WY}}{\rho_f U_w^2},\ \ Nu_X=\dfrac{Xq_W}{k_f(T_W-T_\infty)}, \tag{13}$$

Where τ_{wy} and τ_{wx} are the shear stresses surface in the Y – and X – directions.

$$\tau_{WX}=\left[\mu_{hnf}\dfrac{\partial U}{\partial Z}\right]_{Z=0},\ \tau_{WY}=\left[\mu_{hnf}\dfrac{\partial V}{\partial Z}\right]_{Z=0},\ q_W=-k_{hnf}\left(\dfrac{\partial T}{\partial Z}\right)_{Z=0}, \tag{14}$$

By using equations, (13) and (14), one can obtain the alleviate form

$$\sqrt{Re_X}\,C_{fx}=\dfrac{F''(0)}{(1-\phi_{MWC})^{2.5}(1-\phi_{SWC})^{2.5}} \tag{15}$$

$$(X/Y)\sqrt{Re_X}\,C_{fY} = \frac{cG''(0)}{(1-\phi_{MWC})^{2.5}(1-\phi_{SWC})^{2.5}} \qquad (16)$$

$$\frac{Nu_X}{\sqrt{Re_X}} = -\frac{k_{hnf}}{k_f}\Theta'(0). \qquad (17)$$

3. Analytical method for solution:

3.1. Homotopy perturbation method

Before solving the proposed problem, we first introduce the Homotopy method in this section. This method was introduced by Mr. He in 1998 and has been used to solve the nonlinear ordinary differential equation (ODE). In 2004, he combined this method with the boundary element method and proposed the method of general boundary element [33]. By means of Homotopy perturbation, a series of initial guesses can be evaluated and by a series of auxiliary parameters, a series of answers can be obtained, which converge to the exact answer. This method utilizes features such as freedom of action in choosing the initial function and linear operator. By using the same freedom of action and initial choices, a complex nonlinear problem is solved and transformed into smaller and simpler linear problems. Another advantage of this method is the controllability of the convergence area, which is the most significant feature of this method in comparison with other methods. Some of the articles about Homotopy method are in references [34-35].

To explain the basic ideas of this manner, we consider the following nonlinear differential equation:

$$A(u) - f(r) = 0, \quad r \in \Omega, \qquad (18)$$

With the boundary condition of:

$$B(u, \frac{\partial u}{\partial n}), \quad r \in \Gamma, \qquad (19)$$

Where *A* is a universal differential operator, *B* a boundary operator, f(r) a known analytical function, (Γ) is the boundary of the domain (Ω) and ($\partial u/\partial n$) denotes differentiation along the normal

engrossed outwards from (Ω). *A* can be segregated into two sectors which are *L* and *N*, where *L* is the linear sector and *N* is nonlinear sector. Eq. (18) can therefore be rewritten as follows:

$$-f(r) + N(u) + L(u) = 0, \tag{20}$$

Homotopy perturbation structure is displayed as follows:

$$H(v,p) = p(N(v) - f(r)) + L(u_0) + L(v) + pL(u_0) = 0, \tag{21}$$

Where,

$$v(r,p): \quad \Omega \times [0,1] \to R, \tag{22}$$

In Eq. (21), $p \in [0, 1]$ is an embedding parameter and u_0 is the first approximation that satisfies the boundary condition. We can assume that the solution of Eq. (21) can be written as a power series in *P*, as following:

$$v = v_0 + pv_1 + p^2 v_2 + ... \tag{23}$$

And the best estimation for solution is:

$$u = \lim_{p \to 1} v = v_0 + v_1 + v_2 + ... \tag{24}$$

3.2. Solution with HPM method

In this segment, solving non-linear ordinary differential equations (9) – (11) under the boundary condition (12) are examined using HPM method at ($\phi_{Swc} = \phi_{Mwc} = 0.1, \Pr = 6.2, C = 0.5, \delta = 0.5, n = 1$). According to the HPM, we construct a homotopy presume the solution of Eqs. (9)- (11) has the form:

$$H(F,p) = \left(F''' - F'\right)\left(1-p\right)$$

$$+P\left(\cfrac{1}{\left(1-\phi_{MWC}\right)^{2.5}\left(1-\phi_{SWC}\right)^{2.5}\left[1-\phi_{SWC}\left(\left(1-\phi_{MWC}+\phi_{MWC}\cfrac{\left(\rho C_p\right)_{S_{(MWC)}}}{\left(\rho C_p\right)_f}\right)+\phi_{SWC}\cfrac{\left(\rho C_p\right)_{S_{(SWC)}}}{\left(\rho C_p\right)_f}\right)\right]}F'''\right.$$

$$+cGF''\text{-}F'^2 + FF'' + 1) = 0$$

$$H(G,p) = \left(G''' - G'\right)\left(1-p\right)$$

$$+P\left(\cfrac{1}{\left(1-\phi_{MWC}\right)^{2.5}\left(1-\phi_{SWC}\right)^{2.5}\left[1-\phi_{SWC}\left(\left(1-\phi_{MWC}+\phi_{MWC}\cfrac{\left(\rho C_p\right)_{S_{(MWC)}}}{\left(\rho C_p\right)_f}\right)+\phi_{SWC}\cfrac{\left(\rho C_p\right)_{S_{(SWC)}}}{\left(\rho C_p\right)_f}\right)\right]}G'''\right.$$

$$+FG''+cGG''\text{-}cG'^2 + c) = 0 \tag{25}$$

$$H(\Theta,p) = \left(1-p\right)\left(\Theta'' - \Theta\right)$$

$$+P\left(\cfrac{\cfrac{k_{hnf}}{k_f}}{Pr\left[1-\phi_{SWC}\left(\left(1-\phi_{MWC}+\phi_{MWC}\cfrac{\left(\rho C_p\right)_{S_{(MWC)}}}{\left(\rho C_p\right)_f}\right)+\phi_{SWC}\cfrac{\left(\rho C_p\right)_{S_{(SWC)}}}{\left(\rho C_p\right)_f}\right)\right]}\Theta''+F\Theta'+cG\Theta'\right) = 0$$

We consider $F(\eta)$, $G(\eta)$ and $\Theta(\eta)$ as follows:

$$F(\eta) = F_0(\eta) + F_1(\eta) + \ldots = \sum_{i=0}^{n} F_i(\eta)$$

$$G(x) = G_0(\eta) + G_1(\eta) + \ldots = \sum_{i=0}^{n} G_i(\eta) \tag{26}$$

$$\Theta(x) = \Theta_0(\eta) + \Theta_1(\eta) + \ldots = \sum_{i=0}^{n} \Theta_i(\eta)$$

Substituting Eq. (26), into Eq. (25), and some simplification and rearranging on powers of *P*-terms, we have:

$$p^0 :$$
$$F_0''' - F_0' = 0,$$
$$G_0''' - G_0' = 0, \tag{27}$$
$$\Theta_0'' - \Theta_0 = 0$$

And boundary conditions are:

$x = 0$: $F_0'(0) = 0, F_0(0) = 0, \quad G_0(0) = 0, \quad G_0'(0) = 0, \quad \Theta_0(0) = 1 + \delta \dfrac{k_{hnf}}{k_f} \Theta_0'(0),$

$x \to \infty$: $F_0'(\infty) \to 1, G_0'(\infty) \to 1, \Theta_0(\infty) \to 0$

(28)

And

p^1:

$F_0' - (F_1') + 0.41(F_0''') + F_1''' + G_0(F_0'') - (F_0')^2 F_0 + 1 = 0$

$0.41 G_0''' + G_1''' - (G_1') + G_0' + G_0'' F_0 + (G_0'') G_0 - (G_0'')^2 + 1 = 0$

$-0.81(\Theta_0'') + \Theta_1'' + \Theta_0 - \Theta_1 + F_0(\Theta_0') + \Theta_0' G_0 = 0$

(29)

And boundary conditions are:

$x = 0$: $F_1'(0) = 0, F_1(0) = 0, \quad G_1(0) = 0, \quad G_1'(0) = 0, \quad \Theta_1(0) = 1 + \delta \dfrac{k_{hnf}}{k_f} \Theta_1'(0),$

$x \to \infty$: $F_1'(\infty) \to 1, G_1'(\infty) \to 1, \Theta_1(\infty) \to 0$

(30)

Solving Eqs. (27) and (29) with boundary conditions, we have:

$F_0(\eta) = 0$

$G_0(\eta) = 0$

$\Theta_0(\eta) = e^{-\eta}$

(31)

$F_1(\eta) = \dfrac{\eta e^{\eta} - e^{\eta} + 1}{e^{\eta}}$

$G_1(\eta) = \dfrac{\eta e^{\eta} - e^{\eta} + 1}{e^{\eta}}$

(32)

$\Theta_1(\eta) = e^{-\eta} + \dfrac{4 \times 10^{-10} (2.5 \times 10^9 + 2.4\eta \times 10^8)}{e^{\eta}}$

The terms $\Theta(\eta)$, $G(\eta)$ and $F(\eta)$ when $i \geq 2$ are too large that is forenamed graphically. The solution of this equation, when $p \to 1$, will be as follows:

$F(\eta) = F_0(\eta) + F_1(\eta) + \ldots + F_{10}(\eta)$

$G(\eta) = G_0(\eta) + G_1(\eta) + \ldots + G_{10}(\eta)$

$\Theta(\eta) = \Theta_0(\eta) + \Theta_1(\eta) + \ldots + \Theta_{10}(\eta)$

4. Results and discussions:

The differential systems consisting of Eqs. (9) - (11) have been solved via analytical manner (Homotopy Perturbation Method (HPM)) in Matlab-14 software. Graphical analysis of the impressive parameters like: Prandtl number (Pr), Thermal slip parameter (δ), CNTs volume fraction (ϕ) is precisely checked on the profiles of velocity and temperature for disparate carbon nano-tubes (MWCNT - SWCNT). (See Figures 5-8). In order to achieve more accurate outputs in line with the objectives of this paper and to validate the results in the simulation section, a precise comparison has been made in this research. The comparison between the analytical (HPM) and numerical (4th-5th-order Runge–Kutta–Fehlberg) methods for base fluids ($C_2H_6O_2$, H_2O and Engine oil) and various carbon nanotubes in this essay shows the high accuracy of the present simulation and the discussed results. (See figures 2-4) Likewise, in order to survey the perspicuity of the present probe, we evaluate HPM solution with the output of prior essay published by Ref (Dinarvand et al. [30]) for titanium dioxide and Cu-H_2O Nano liquid. The comparisons are tested in Table 2. The low mistake in this table displays the high punctuality of the present simulation.

The choice of base liquid has a significant impact on the graphs of velocity and temperature. This research shows that the highest graphs of velocity and temperature is for Engine oil base fluid. Also, the lowest graphs of velocity and temperature is for water base fluid. (See figure 5). Figure 6(a-d) shows the mutations in the velocity profile ($f'(\eta)$) along the x axis for diverse amounts of the nanoparticles' volume fraction parameter (ϕ). This figure actually depicts the behavior of the hybrid Nano liquid and Nano liquid flow for different carbon nanotubes (SWCNT-MWCNT) at saddle points and nodal points. Based on observations, it was determined that the profile $f'(\eta)$ is a decreasing function of ϕ at both dots. In addition, it should be noted that the velocity profile $f'(\eta)$ provides a larger boundary layer thickness for hybrid Nano fluids than Nano fluids. Furthermore, multi-walled carbon nanotubes are more effective than single-walled nanotubes in increasing the velocity profile. The impact of the nanoparticles' volume fraction (ϕ) on the velocity of the Nano fluids and hybrid Nano fluids along the Y axis is shown in Figure 7(a-d). In these figures, a diverse behaviour is observed for the velocity profile at saddle and nodal dots. It is as well as clear that the velocity graph along the Y axis is, similarly to $f'(\eta)$, a decreasing function of ϕ at both points, but with the difference

that the velocity profile at the saddle point has first an increasing tend up to the point η_m. In fact, η_m is the intersection dot of the velocity graph for several values of ϕ. In addition, it can be seen from these figures that the velocity profile $G'(\eta)$ has a lower boundary layer thickness than the velocity profile along the x axis ($f'(\eta)$). It is noteworthy that the velocity graph $G'(\eta)$ provides a lower boundary layer thickness at the saddle point for hybrid Nano fluids than Nano fluids. The impact of the nanoparticles' volume fraction parameter ϕ on the temperature profile $\Theta(\eta)$ for various carbon nanotubes (SWCNT-MWCNT) is shown in Figure 8(a-d). As expected, the straight relevance between ϕ and thermal conductivity growths the thickness of the heat and temperature layer at both saddle and nodal points. Furthermore, due to the higher thermal conductivity of the SWCNT nano-particles, the growth in temperature in these nano-particles is more than MWCNT. It is noteworthy that the temperature profile $\Theta(\eta)$ provides a larger thermal boundary layer thickness at both points for hybrid Nano fluids than Nano fluids. The temperature distribution without considering the thermal slippage parameter shows an increasing curve for Nano fluids and hybrid Nano fluids. (See Figure 8 b-c). For better visualization, the effect of the thermal slippage parameter is evident in Figure 7(e). It is deduced from this form that high temperature decreases with increasing thermal slippage parameter. In addition, the behaviour of the Pr number on the profile $\Theta(\eta)$ implies that $\Theta(\eta)$ declines for a major Pr number. Indeed, enhancing the Pr number corresponds to a diminution in the thermal permeability coefficient (α), which declines the temperature. (See Figure 8 f). Changes in skin friction and Nusselt number for diverse volume fractions of nanoparticles ϕ for Nano fluids containing carbon nanotubes (SWCNT-MWCNT) are depicted in Tables (2-4). Our outcome demonstrate that heat transfer and surface drag force rate are enhanced linearly for larger estimation of Nanoparticle volume fraction. Additionally, the comparison between (SWCNT-MWCNT) Nano liquids in the actual simulation displays that MWCNT nano-particles have higher crust friction coefficient (Cf) than SWCNT nano-particles.

5. Conclusions:

In this research the specification of 3-dimensional flow stagnation dot of hybrid Nano liquids passing through circular cylinder with sinusoidal radius is analyzed. Plus, the influence of the impressive parameters is precisely studied on the graphs of velocity and temperature for diverse carbon nanotubes (SWCNT-MWCNT). Outcomes displayed that:

- That the velocity profile provides a larger boundary layer thickness for hybrid Nano fluids than Nano fluids.

- Multi-walled carbon nanotubes are more effective than single-walled carbon nanotube in increasing the velocity profile.

- The SWCNT carbon nanotube, due to their premier thermal conductivity, have a better the temperature than MWCNT carbon nanotube.

- The temperature distribution without considering the thermal slippage parameter shows an increasing curve for Nano fluids and hybrid Nano fluids.

- That heat transfer and surface drag force rate are enhanced linearly for larger estimation of Nanoparticle volume fraction.

In the long run, it will be beheld that the nano-particle kind and Nano liquid base is an significant factor in the heating and cooling activities.

References:

[1] Yazid, M., Sidik, N., Yahya, W., Heat and mass transfer characteristics of carbon nanotube nanofluids: A review, *Renewable and Sustainable Energy Reviews*, 80 (2017) 914-941.

[2] Hatami, M., Toxicity assessment of multi-walled carbon nanotubes on Cucurbita pepo L. under well-watered and water-stressed conditions. *Ecotoxicology and Environmental Safety*, 142 (2017) 274-283.

[3] Zhan, M., Pan, G., Wang, Y., Kuang, T., Zhou, F., Ultrafast carbon nanotube growth by microwave irradiation, *Diamond and Related Materials*, 77 (2017) 65-71.

[4] Farooq, S., Hayat, T., Alsaedi, A., Asghar, S., Mixed convection peristalsis of carbon nanotubes with thermal radiation and entropy generation, *Journal of Molecular Liquids*, 250 (2018) 451-467.

[5] Omidi, M. J., ShayanMehr, M., Improving the dispersion of SWNT in epoxy resin through a simple Multi-Stage method, *Journal of King Saud University - Science*, 31 (2019) 202-208.

[6]   Abdallah, S. R., Saidani-Scott, H., Abdellatif, O.E., Performance analysis for hybrid PV/T system using low concentration MWCNT (water-based) nanofluid. *Solar Energy*, 181 (2019) 108-115.

[7]   Rezakazemi, M., Darabi, M., Soroush, E., Mesbah, M., CO_2 absorption enhancement by water-based nanofluids of CNT and SiO_2 using hollow-fiber membrane contactor. *Separation and Purification Technology*, 210 (2019) 920-926.

[8]   Benos, L.Th., Karvelas, E.G., Sarris, I.E., A theoretical model for the magnetohydrodynamic natural convection of a CNT-water nanofluid incorporating a renovated Hamilton-Crosser model. *International Journal of Heat and Mass Transfer*, 135 (2019) 548-560.

[9]   IiJima, S., Helical microtubules of graphitic carbon. *Nature*, 354 (1991) 56-58.

[10]   A. Moradi, D. Toghraie, A. H. M. Isfahani, A. Hosseinian, An experimental study on MWCNT–water nanofluids flow and heat transfer in double-pipe heat exchanger using porous media, *J Therm Anal Calorim* 137 (2019) 1797-1807. https://doi.org/10.1007/s10973-019-08076-0

[11]   Chen, W., Zou, C., Li, X., Hao, L., Application of recoverable carbon nanotube nanofluids insolar desalination system: An experimental investigation. *Desalination*, 451 (2019) 92-101.

[12]   Choi, T.J., Jang, S.P., Kedziersk, M.A., Effect of surfactants on the stability and solar thermal absorption characteristics of water-based nanofluids with multi-walled carbon nanotubes. *International Journal of Heat and Mass Transfer*, 122 (2018) 483-490.

[13]   Selimefendigil, F., Öztop, H.F., Corrugated conductive partition effects on MHD free convection of CNT-water nanofluid in a cavity. *International Journal of Heat and Mass Transfer*, 129 (2019) 265-277.

[14]   Mahbubul, I.M., Khan, M.M.A., Ibrahim, N.I., Ali, H.M., Sulaiman, F.A.A., Carbon nanotube nanofluid in enhancing the efficiency of evacuated tube solar collector. *Renewable Energy*, 121 (2018) 36-44.

[15]   A. Hussanan, M. Qasim, Zhi-M. Chen, Heat transfer enhancement in sodium alginate based magnetic and non-magnetic nanoparticles mixture hybrid nanofluid, *Physica A: Statistical Mechanics and its Applications* (2020), 123957. https://doi.org/10.1016/j.physa.2019.123957

[16]   Taherian, H., Alvarado, J.L., Languri, E.M., Enhanced thermophysical properties of multiwalled carbon nanotubes based nanofluids. Part 1: Critical review. *Renewable and Sustainable Energy Reviews*, 82 (2018) 4326-4336.

[17]   Wang, R., Xie, L., Hameed, S., Wang, C., Ying, Y., Mechanisms and applications of carbon nanotubes in terahertz devices: A review. *Carbon*, 132 (2018) 42-58.

[18]   M. Gholinia, S. A. H. Kiaeian Moosavi, M. Pourfallah, S. Gholinia & D. D. Ganji (2019) A numerical treatment of the $TiO_2/C_2H_6O_2$–H_2O hybrid base nanofluid inside a porous cavity under the impact of shape factor in MHD flow, *International Journal of Ambient Energy*, https://doi.org/10.1080/01430750.2019.1614996

[19]   Ahmadpour, A.S.A., Hajmohammadi, M.R., Thermal design improvement of a double-layered microchannel heat sink by using multi-walled carbon nanotube (MWCNT) nanofluids with non-Newtonian viscosity. *Applied Thermal Engineering*, 147 (2019) 205-215.

[20] Loulijat, H., Koumina, A., Zerradi, H., The effect of the thermal vibration of graphene nanosheets on viscosity of nanofluid liquid argon containing graphene nanosheets. *Journal of Molecular Liquids*, 276 (2019) 936-946.

[21] T. Tayebi, H. F. Öztop, Entropy production during natural convection of hybrid nanofluid in an annular passage between horizontal confocal elliptic cylinders, *International Journal of Mechanical Sciences*, 171 (2020) 105378.

[22] Syam Sundar, L., Singh, M.K., Sousa, A.C.M., Turbulent heat transfer and friction factor of nanodiamond-nickel hybrid nanofluids flow in a tube: An experimental study. *International Journal of Heat and Mass Transfer*, 117 (2018) 223-234.

[23] Minea, A.A., Maghlany, W.M.E., Influence of hybrid nanofluids on the performance of parabolic trough collectors in solar thermal systems: Recent findings and numerical comparison. *Renewable Energy*, 120 (2018) 350-364.

[24] Bellos, E., Tzivanidis, C., Thermal analysis of parabolic trough collector operating with mono and hybrid nanofluids. *Sustainable Energy Technologies and Assessments*, 26 (2018) 105-115.

[25] Huminic, G., Huminic, A., The heat transfer performances and entropy generation analysis of hybrid nanofluids in a flattened tube. *International Journal of Heat and Mass Transfer*, 119 (2018) 813-827.

[26] T. Hayat, M. W. Ahmada, M. Ijaz Khana, A. Alsaedi, Entropy optimization in CNTs based nanomaterial flow induced by rotating disks: A study on the accuracy of statistical declaration and probable error, *Computer Methods and Programs in Biomedicine*, 184 (2020) 105105. https://doi.org/10.1016/j.cmpb.2019.105105

[27] T.Hayat, Sohail A.Khan, M.Ijaz Khan, A.Alsaedi, Irreversibility characterization and investigation of mixed convective reactive flow over a rotating cone, *Computer Methods and Programs in Biomedicine*, 185 (2020) 105168. https://doi.org/10.1016/j.cmpb.2019.105168

[28] T.Hayat, F.Shah, A.Alsaedi, B.Ahmad, Entropy optimized dissipative flow of effective Prandtl number with melting heat transport and Joule heating, International Communications in Heat and Mass Transfer, 111 (2020) 104454. https://doi.org/10.1016/j.icheatmasstransfer.2019.104454

[29] M.Gholinia, M.E.Hoseini, S. Gholinia, A numerical investigation of free convection MHD flow of Walters-B nanofluid over an inclined stretching sheet under the impact of Joule heating, *Thermal Science and Engineering Progress*, 11 (2019) 272-282. https://doi.org/10.1016/j.tsep.2019.04.006

[30] Dinarvand, S., Hosseini, R., Damangir, E., & Pop, I., Series solutions for steady three-dimensional stagnation point flow of a nanofluid past a circular cylinder with sinusoidal radius variation . *Meccanica*, 48 (2013) 643-652.

[31] Tiwari R.K., Das M.S., Heat transfer augmentation in a two-sided lid-driven differentially heated square cavity utilizing nanofluids. *Int J Heat Mass Transf*, 50 (2007) 2002–2018.

[32] Bachok N., Ishak A., Nazar R., Pop I., Flow and heat transfer at a general three-dimensional stagnation point in a Nano fluid. *Physica B*, 405 (2010) 4914–4918.

[33]   He, J.H., Comparison of homotopy perturbation method and homotopy analysis method. *Appl Math Comput*, 156 (2004) 527-539.

[34]   Sajid, M., Hayat, T., Comparison of HAM and HPM solutions in heat radiation equations, *International Communications in Heat and Mass Transfer*, 36 (2009) 59-62.

[35]   Shqair, M., Solution of different geometries reflected reactors neutron diffusion equation using the homotopy perturbation method. *Results in Physics*, 12 (2019) 61-66.

[36]   Mohammad, R., Kandasamy, R., Nanoparticle shapes on electric and magnetic force in water, ethylene glycol and engine oil based Cu, Al_2O_3 and SWCNTs. *Journal of Molecular Liquids*, 237 (2017) 54-64.

(a)

M

N

O

Hybrid Nano-Fluid

(b)

x

wall

Free steam

y

Nodal Attachment Point
Points(M and O)

x

y

Separation line

Saddle Attachment Point
Point (N)
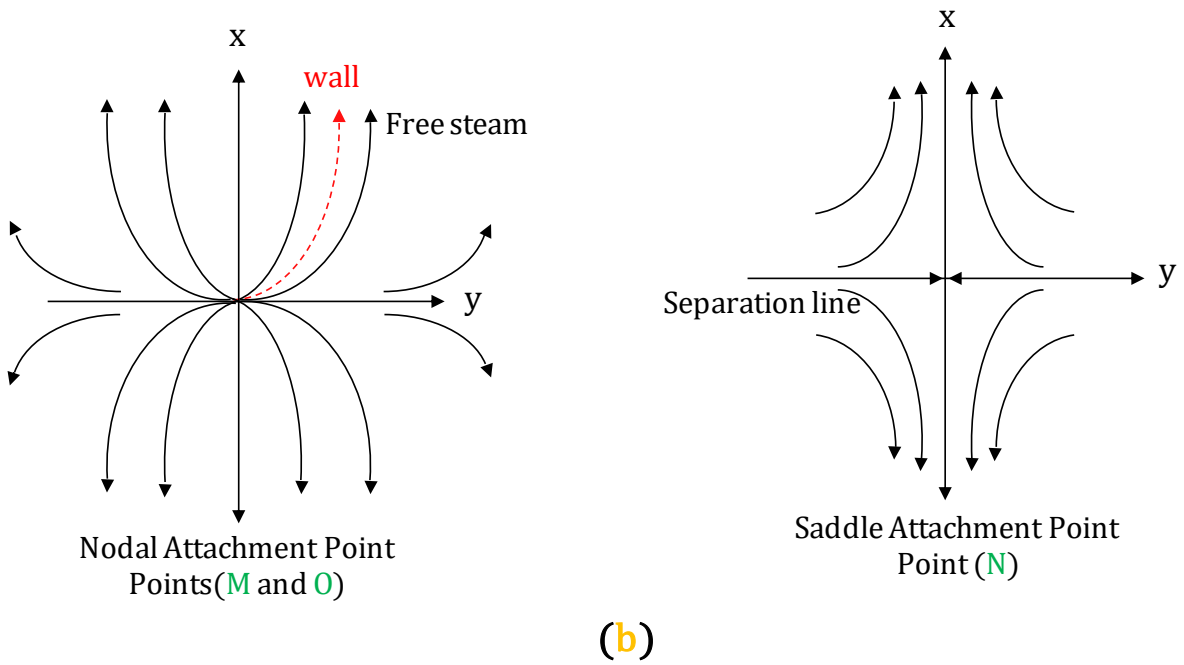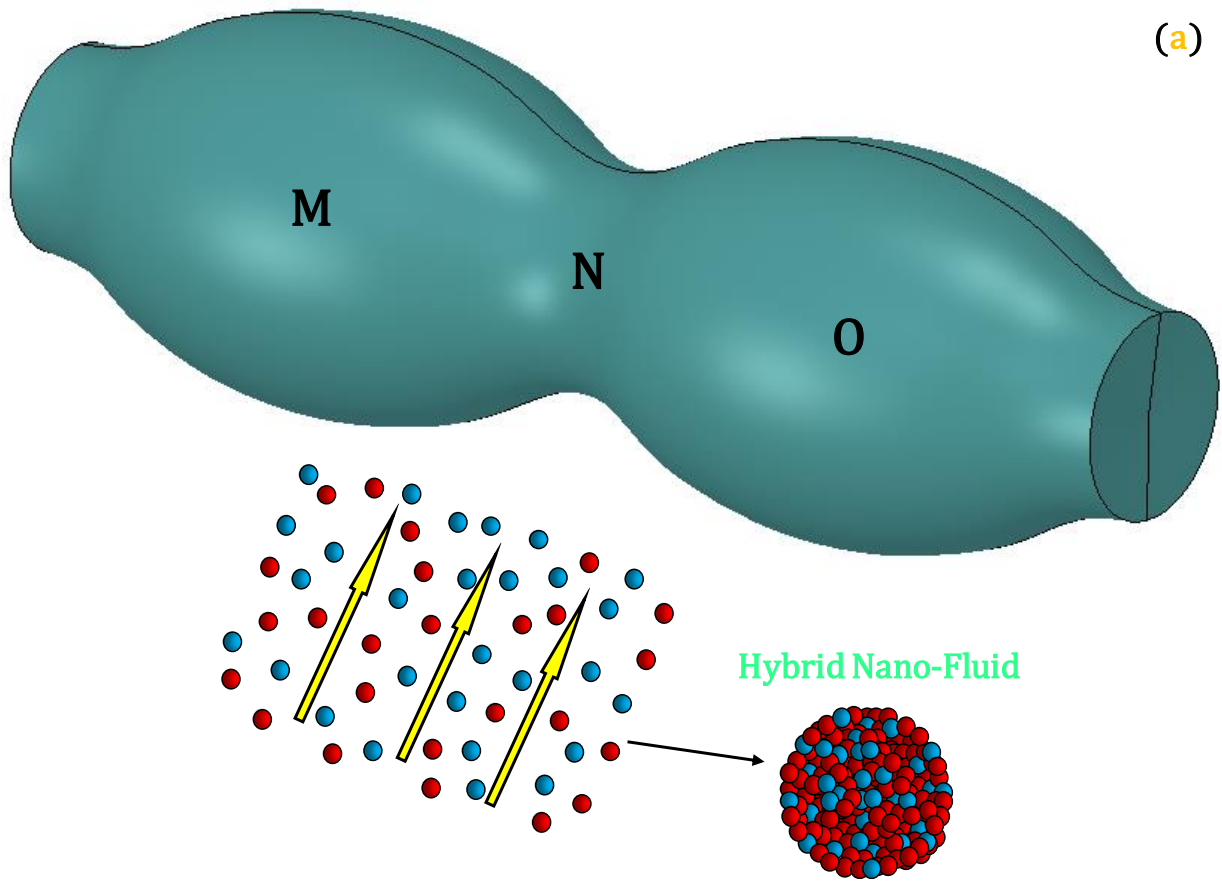
Fig. 1. Pattern of the issue.
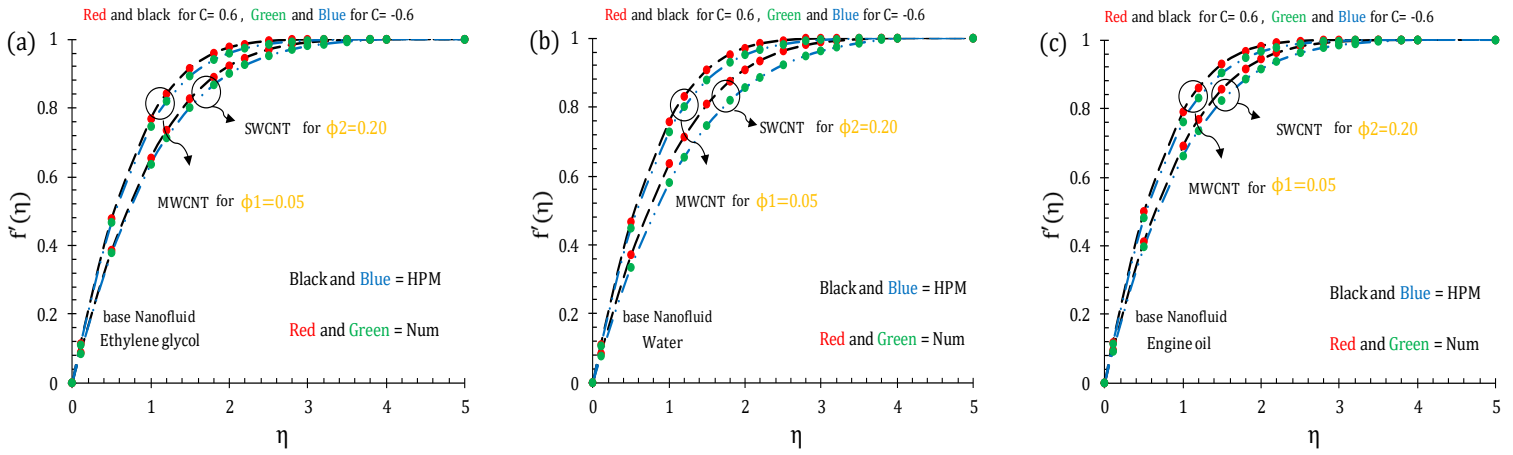
Fig. 2. Comparison of the velocity profile between HPM and Numerical Method for base liquids ($C_2H_6O_2$, H_2O and Engine oil) and various carbon nanotubes
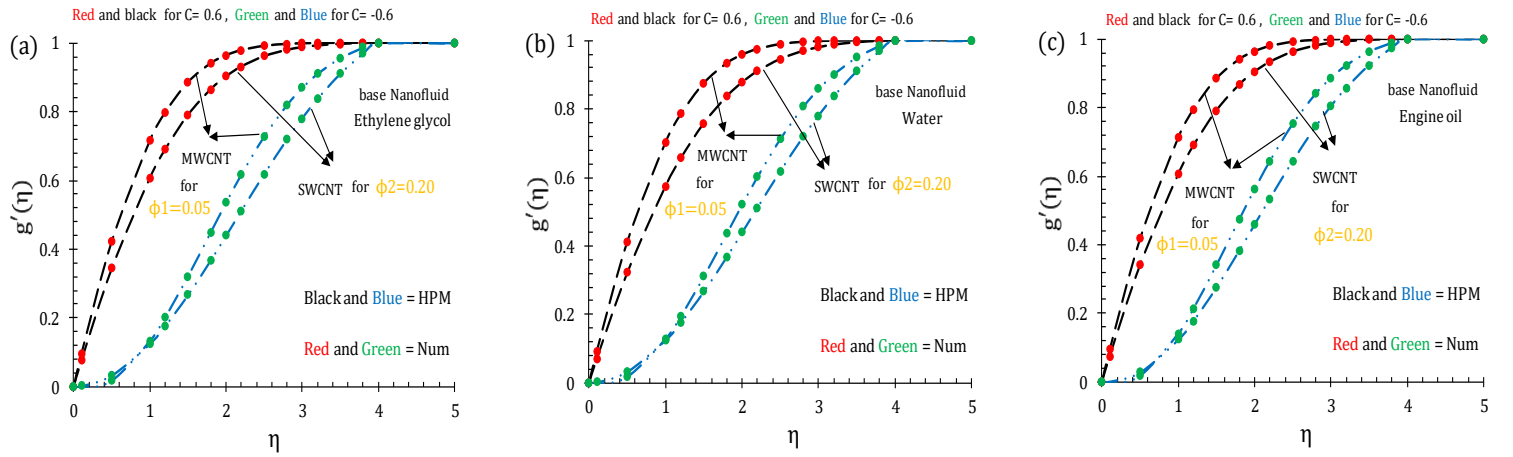

Fig. 3. Comparison of the velocity profile between HPM and Numerical Method for base liquids ($C_2H_6O_2$, H_2O and Engine oil) and various carbon nanotubes
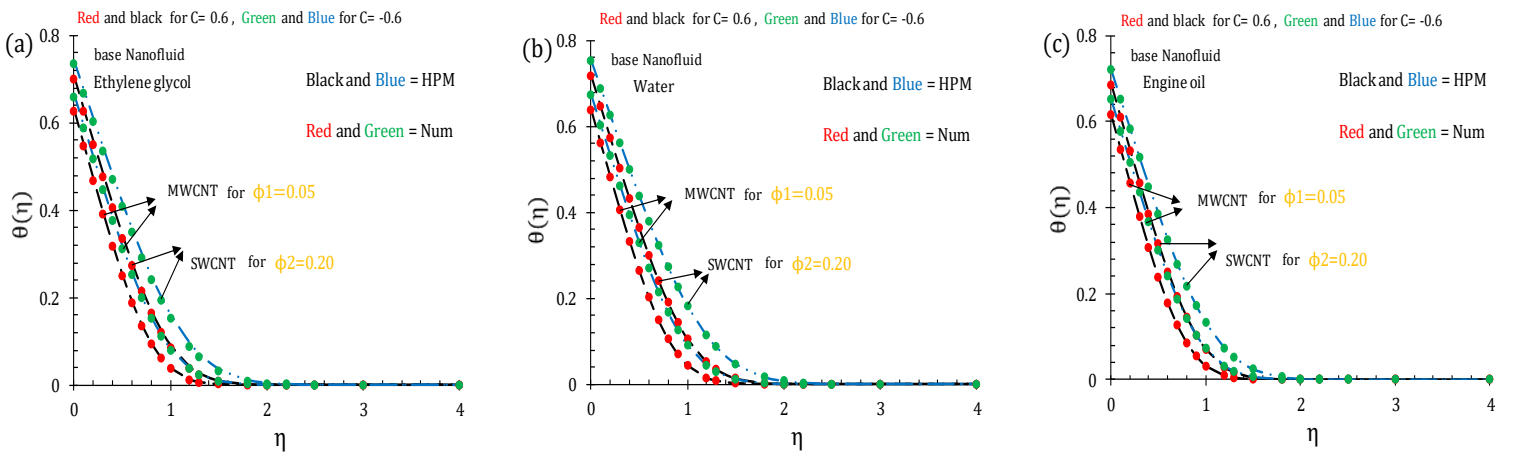

Fig. 4. Comparison of the temperature profile between HPM and Numerical Method for base liquids ($C_2H_6O_2$, H_2O and Engine oil) and various carbon nanotubes

(a) δ=0.5, C=0.5

base Nanofluid

Water -Ethylene glycol- Engine oil

Black: SWCNT

Red: MWCNT

(b) δ=0.5, C=0.5

base Nanofluid

Water -Ethylene glycol- Engine oil

Black: SWCNT

Red: MWCNT

(c) δ=0.5, C=0.5

Black: SWCNT

Red: MWCNT

base Nanofluid

Water -Ethylene glycol- Engine oil
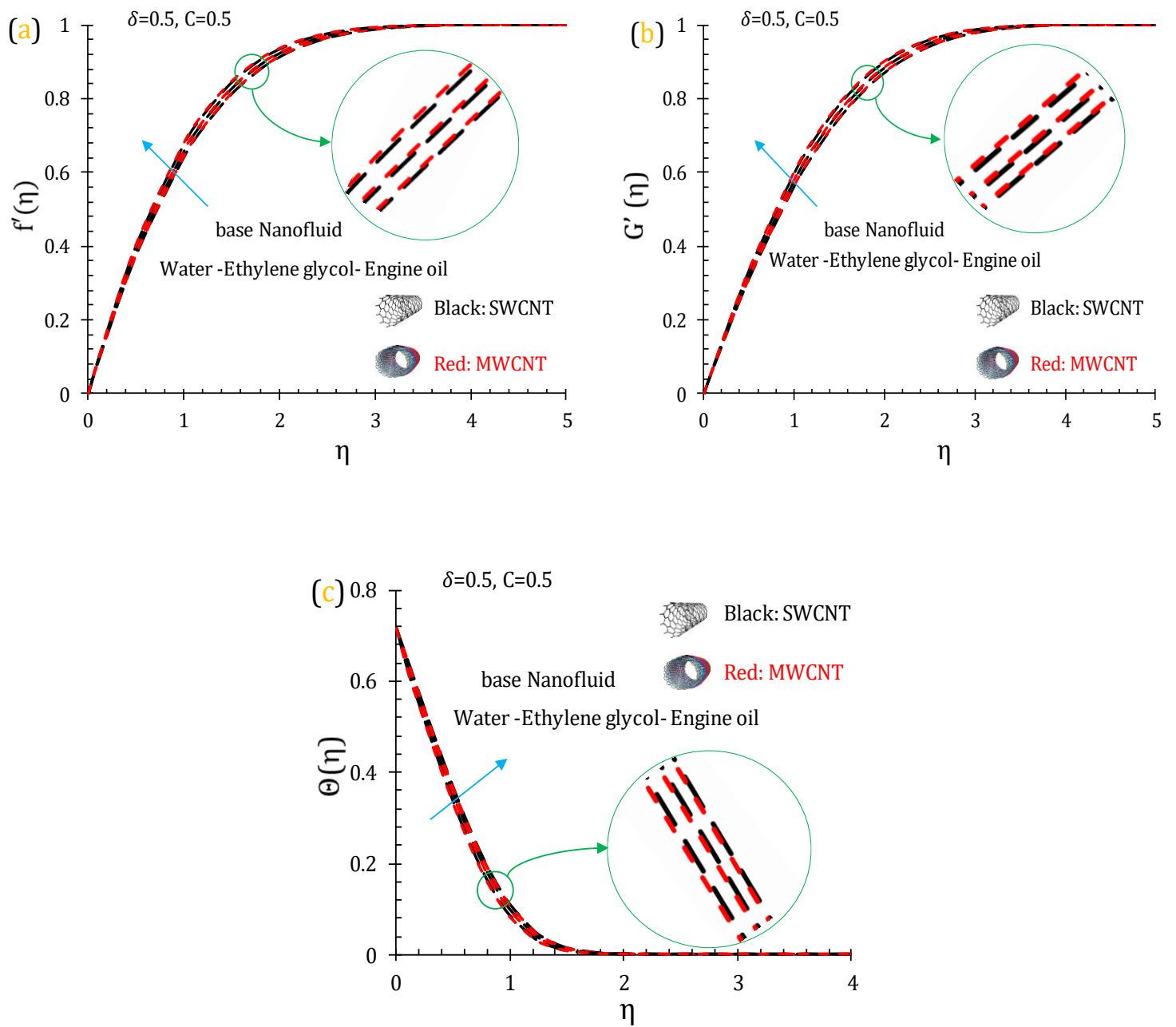
Fig. 5. Comparison between the base fluids ($C_2H_6O_2$, H_2O and Engine oil) for various carbon nanotubes.
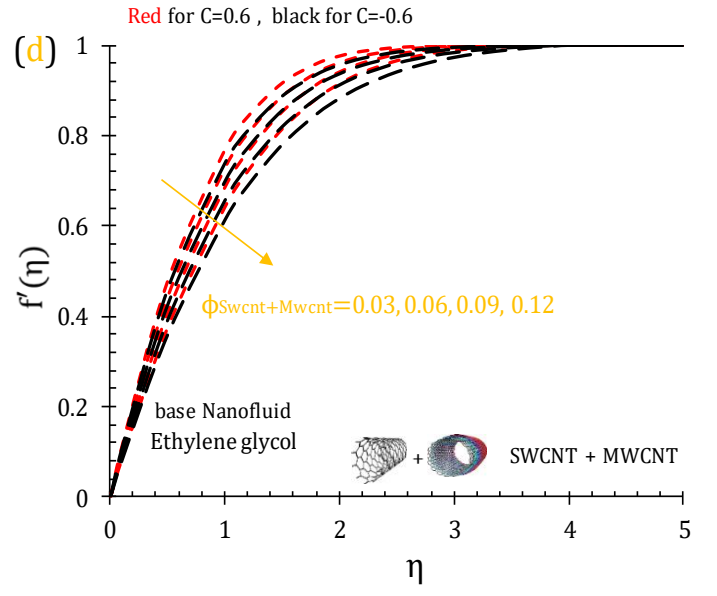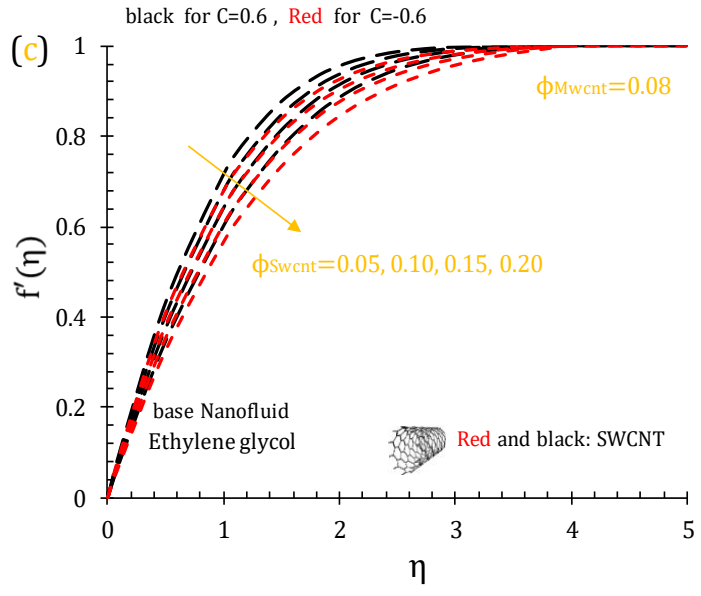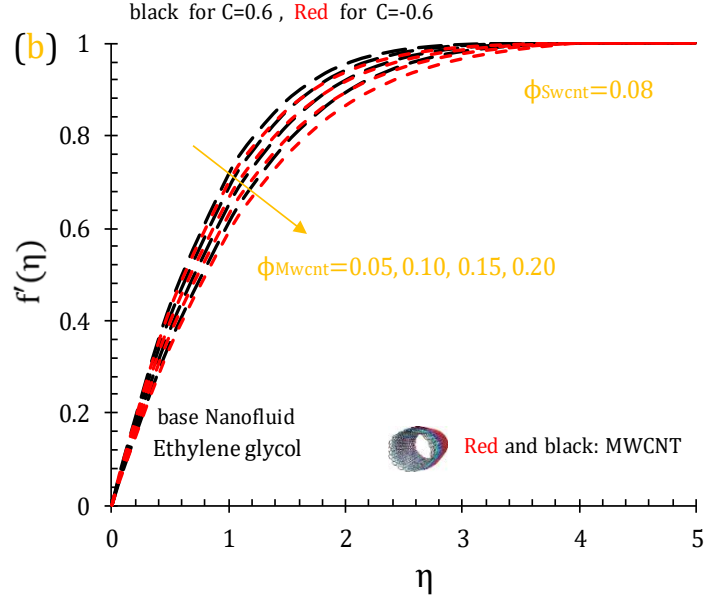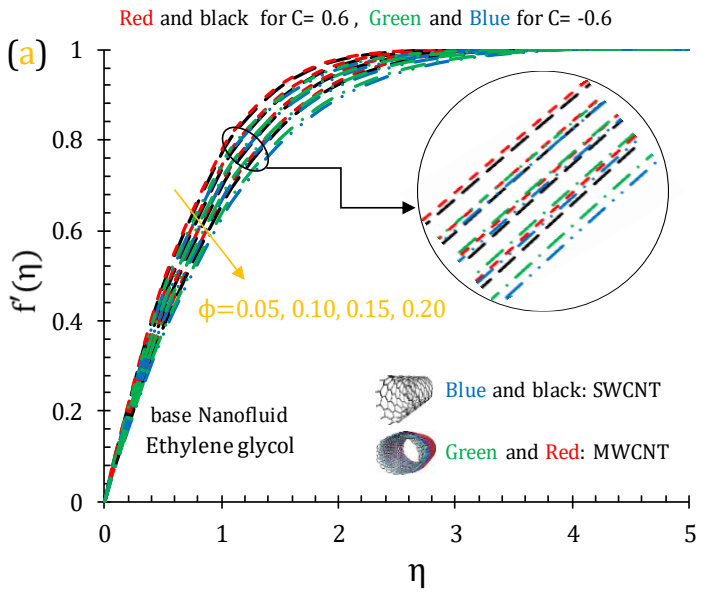
Figs. 6(a-d). Impact of φ on f'(η) for the hybrid Nano fluid and Nano fluid flow.
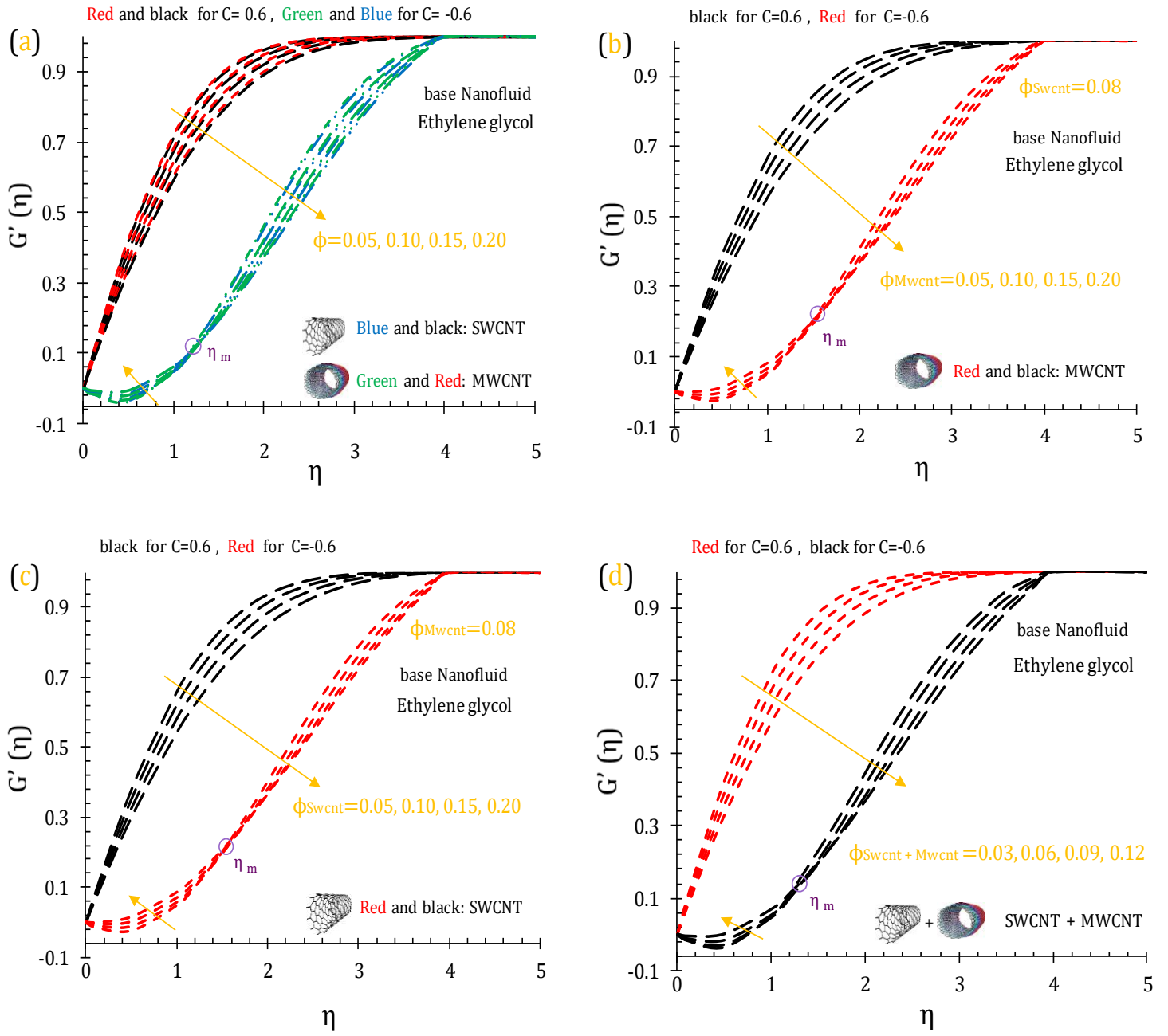
Figs. 7(a-d). Impact of ϕ on G'(η) for the hybrid Nano fluid and Nano fluid flow.

(a) Red and black for C= 0.6, Green and Blue for C= -0.6

base Nanofluid
Ethylene glycol

ϕ=0.05, 0.10, 0.15, 0.20

Blue and black: SWCNT
Green and Red: MWCNT

(b) black for C=0.6, Red for C=-0.6

base Nanofluid
Ethylene glycol

ϕ_{Swcnt}=0.08
δ=0.0

ϕ_{Mwcnt}=0.05, 0.10, 0.15, 0.20

Red and black: MWCNT

(c) black for C=0.6, Red for C=-0.6

base Nanofluid
Ethylene glycol

ϕ_{Mwcnt}=0.08
δ=0.0

ϕ_{Swcnt}=0.05, 0.10, 0.15, 0.20

Red and black: SWCNT

(d) Red for C=0.6, black for C=-0.6

base Nanofluid
Ethylene glycol

$\phi_{Swcnt+Mwcnt}$=0.03, 0.06, 0.09, 0.12
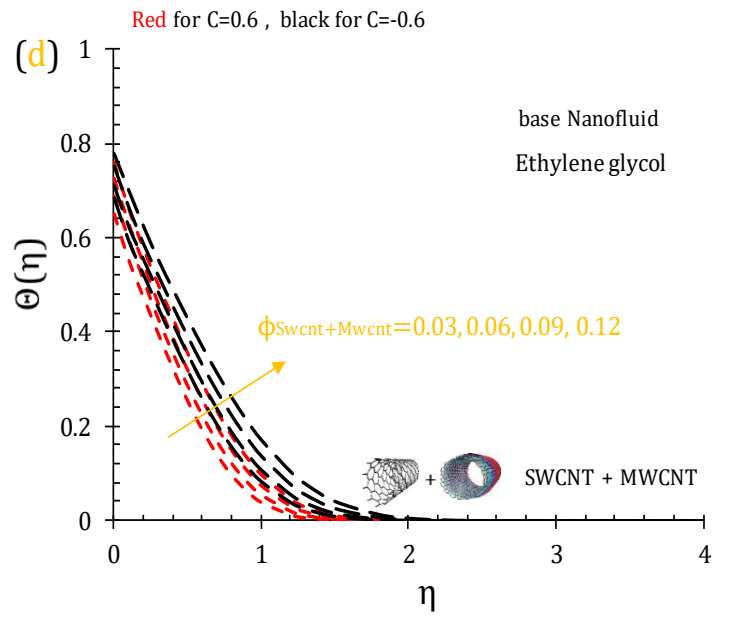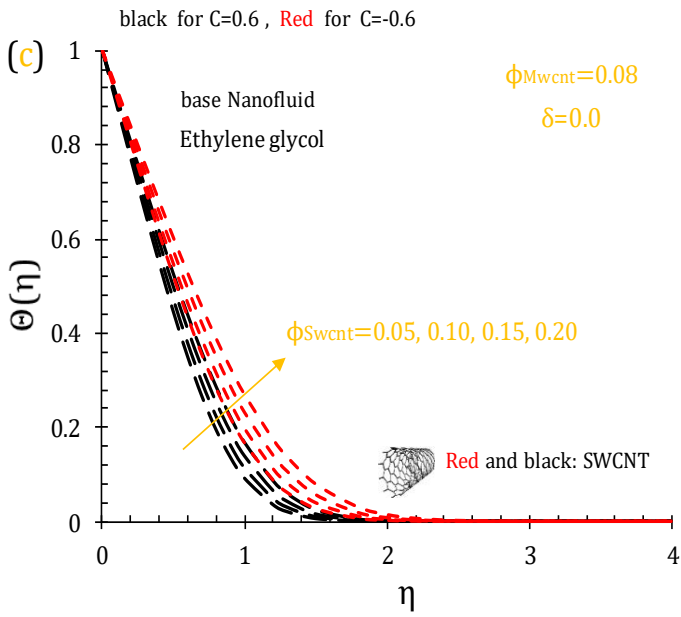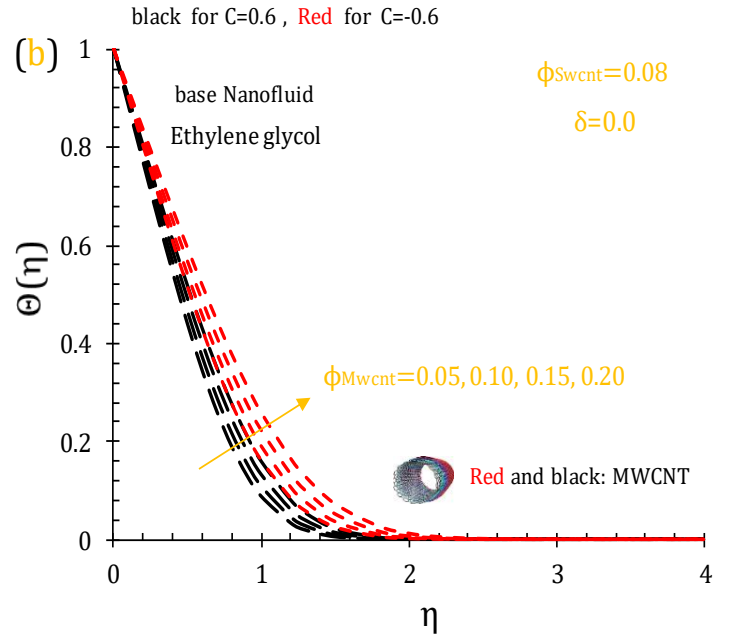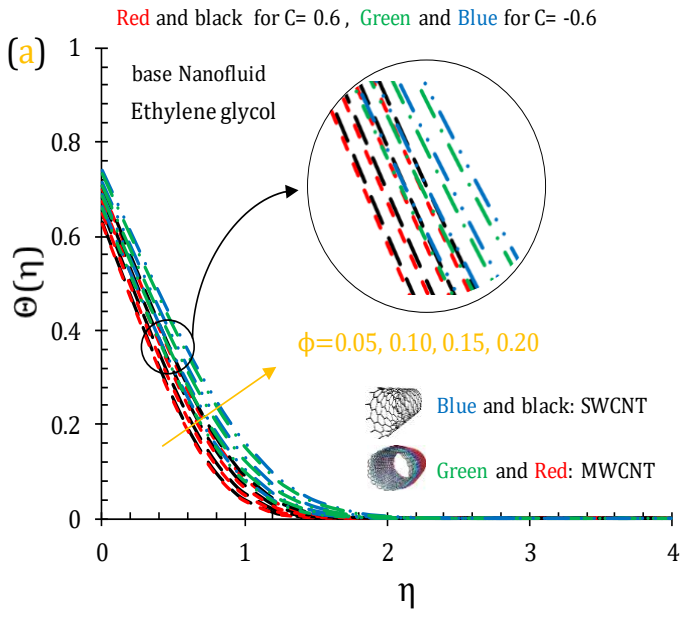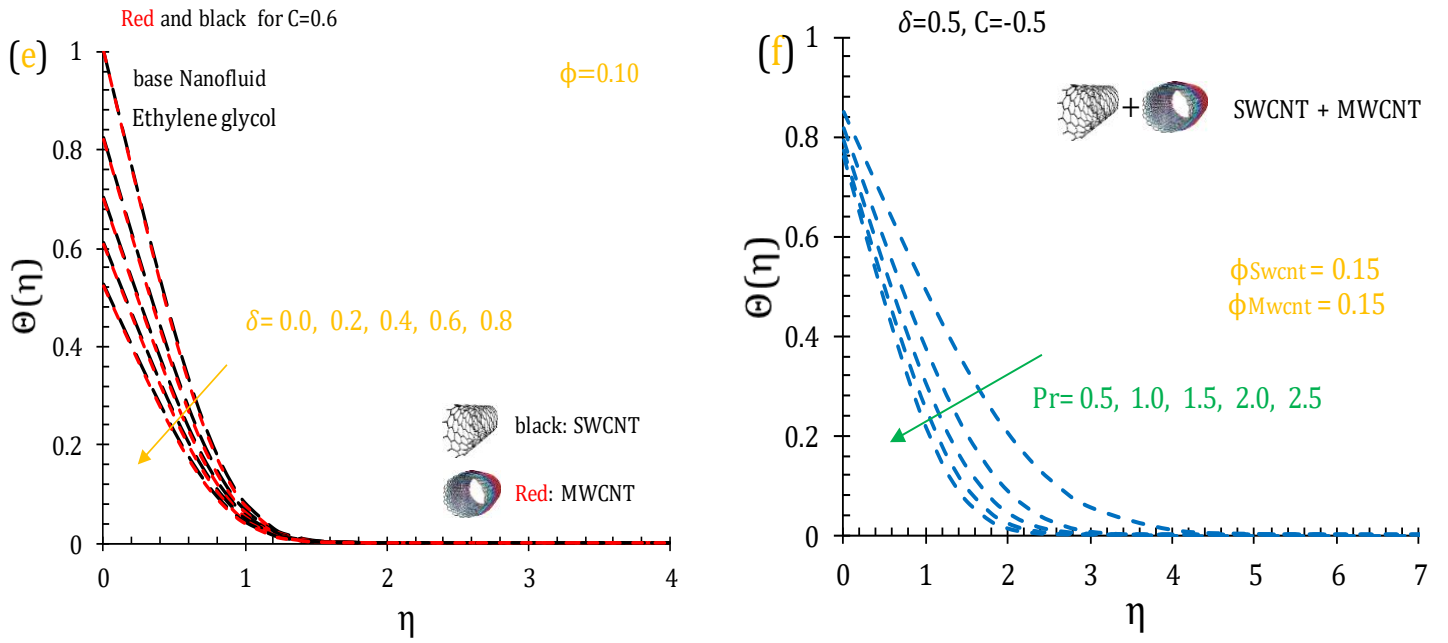
SWCNT + MWCNT

Figs. 8(a-f). Impact of ϕ, δ and Pr on Θ(η) for the hybrid Nano fluid and Nano fluid flow.

Table.1. Thermo-physical properties of ($C_2H_6O_2$, H_2O and Engine oil) and the Nanotubes (SWCNT - MWCNT) [18, 26, 36].

Base fluid and Nanotubes	C_p ($\frac{J}{kg}.K$)	ρ(kg/m³)	k ($\frac{W}{m}.K$)	$\alpha \times 10^{-7}$ (m²/s)
Ethylene glycol ($C_2H_6O_2$)	2430	1115	0.253	0.938
Pure water(H_2O)	4179	997.1	0.613	1.470
Engine oil	1910	884	0.144	0.850
SWCNT	425	2600	6600	59728.50
MWCNT	796	1600	3000	23555.27

Table.2. Match of the amounts of skin friction coefficient (Cf) and the local Nusselt number (Nu) when ($\Phi_{MWC}=\Phi_{Dinarvand}$) and $\delta=0.0$, $\Phi_{SWC}=0.0$

	$\Phi_{MWC}=\Phi_1$	$\sqrt{Re_x}C_{fx}$			$x/y\sqrt{Re_x}C_{fy}$			$Nu_x/\sqrt{Re_x}$		
		HAM	HPM	Error	HAM	HPM	Error	HAM	HPM	Error
	0.00	1.2681	1.2682	0.0001	0.4993	0.4992	0.0001	1.3301	1.3300	-0.0001
Cu	0.10	1.9387	1.9385	-0.0002	0.7630	0.7629	-0.0001	1.6185	1.6183	-0.0002
	0.20	2.6968	2.6970	0.0002	1.0617	1.0615	-0.0002	1.9293	1.9290	-0.0003
	0.00	1.2681	1.2682	0.0001	0.4993	0.4991	-0.0002	1.3301	1.3299	-0.0002
Tio$_2$	0.10	1.6657	1.6659	0.0002	0.6557	0.6556	-0.0001	1.4956	1.4954	-0.0002
	0.20	2.1530	2.1535	0.0005	0.8477	0.8474	-0.0003	1.7386	1.7383	-0.0003

Table.3. Impact of ϕ on skin friction for the hybrid Nano liquid and Nano liquid flow.

Φ_{MWC}	Φ_{SWC}	SWCNT – MWCNT/ Ethylene glycol		SWCNT / Ethylene glycol		MWCNT/ Ethylene glycol	
		$\sqrt{Re_x}C_{fx}$	$x/y\sqrt{Re_x}C_{fy}$	$\sqrt{Re_x}C_{fx}$	$x/y\sqrt{Re_x}C_{fy}$	$\sqrt{Re_x}C_{fx}$	$x/y\sqrt{Re_x}C_{fy}$
0.05	0.05	1.401	0.551	1.330	0.524	1.332	0.525
0.10	0.10	1.550	0.614	1.401	0.551	1.404	0.554
0.15	0.15	1.748	0.690	1.481	0.583	1.489	0.586
0.20	0.20	1.983	0.788	1.572	0.619	1.583	0.624

Table.4. Impact of φ on Nusselt number for the hybrid Nano fluid and Nano fluid flow.

Φ_{MWC}	Φ_{SWC}	SWCNT – MWCNT/ Ethylene glycol	SWCNT / Ethylene glycol	MWCNT/ Ethylene glycol
		$Nu_x/\sqrt{Re_x}$	$Nu_x/\sqrt{Re_x}$	$Nu_x/\sqrt{Re_x}$
0.05	0.05	0.638	0.619	0.620
0.10	0.10	0.674	0.638	0.640
0.15	0.15	0.709	0.657	0.660
0.20	0.20	0.744	0.677	0.680

Nomenclature			
C_f	Skin friction coefficient	Θ	Temperature profile
F'	Velocity profile along X- path	δ	Thermal slip parameter
G'	Velocity profile along Y- path	η	dimensionless variable
k	Thermal conductivity coefficient	$\rho(C_P)_{nf}$	Heat capacity of Nano fluid
Nu	Nusselt number	ρ	Density
Pr	Prandtl number	k_f	Thermal conductivity of liquid
T_w	Wall temperature	k_{nf}	Thermal conductivity of Nano fluid
T_∞	Ambient temperature	k_{hnf}	Thermal conductivity of hybrid Nano fluid
Φ_{MWC}	Nano-particle volume fraction of MWCNT	μ_{hnf}	Viscosity of hybrid Nano liquid
Φ_{SWC}	Nano-particle volume fraction of SWCNT	μ_{nf}	Viscosity of Nano liquid
ν_f	Fluid kinematic Viscosity	α_{hnf}	thermal diffusivity of hybrid Nano liquid
ν_{nf}	Nano fluid kinematic Viscosity	α_{nf}	thermal diffusivity of Nano liquid
ν_{hnf}	Hybrid Nano liquid kinematic Viscosity	$\rho(C_P)_{hnf}$	Heat capacity of hybrid Nano liquid